Audio Engineering Society

Convention Paper

Presented at the 141st Convention
2016 September 29–October 2 Los Angeles, USA

Determining the muzzle blast duration and acoustical energy of quasi-anechoic gunshot recordings

Tushar Routh and Robert C. Maher

Electrical & Computer Engineering, Montana State University, Bozeman, Montana, USA

Correspondence should be addressed to Tushar Routh (tusharrouth@gmail.com)

ABSTRACT

Investigation of gunshot waveforms largely includes analyzing the muzzle blast. Generated by the combustion of gunpowder immediately after firing, these brief duration directional shock waves travel outward in all directions at the speed of sound. Features of these waveforms are analyzed to identify characteristics of a particular shot, for example, the combination of firearm type, ammunition, and orientation. This paper includes measured muzzle blast durations for several common firearms and calculation of the total acoustical energy during the muzzle blast period.

1 Introduction

Acoustic gunshot signals can play an important role in audio forensic investigations involving gunshot analysis. Gunshot signals, captured from some sort of surveillance systems placed near a crime scene, can answer questions which are crucial for a law enforcement investigation [1]. In recent years, many law enforcement agencies have become equipped with audio recording devices that are capable of capturing gunshot audio signals from crime scenes. Audio forensic experts are increasingly being asked to provide their expert opinions before the court based on these recordings [2]. However, the acoustic characteristics of gunshots remain little understood in an objective sense, and therefore may be subject to unscientific physical misunderstanding and subjective interpretation. Moreover, the limitations of commonly available audio recorders can seriously affect reaching a reliable conclusion from the available audio evidence [3].

Gunshots from a typical firearm will result in two different kinds of acoustic disturbances. When fired, the primer initiates combustion of gunpowder, producing hot expanding gas that escapes through the opening of the barrel as the bullet is expelled. This is the *muzzle blast*. The other form of disturbance, a *ballistic shockwave*, occurs when the bullet travels faster than the speed of sound [4].

2 Muzzle Blasts

Although the purpose of using gunpowder is to propel the bullet in the forward direction, it has been found that conventional firearms manage to use only a

fraction of their total blast energy to propel the bullet. The residual energy is lost as heat and in the rapid air displacement after escaping from the muzzle of the firearm, introducing the muzzle blast [5]. If observed carefully, the muzzle blast lasts only for a few milliseconds, propagating in all directions at the speed of the sound. The muzzle blast is directional, commonly exhibiting higher sound pressure in the direction the firearm is pointing and decreasing in amplitude with increasing azimuth [1]. Figure 1 shows an example of the recorded muzzle blast wave generated by a Glock 23 pistol fired in the direction of the recording microphone.

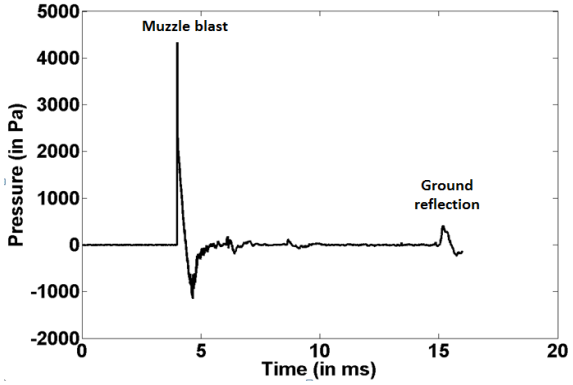

Figure 1: Muzzle blast pressure wave of a Glock 23 gunshot signal recorded on-axis 3 meters from the muzzle (16-bit, 500 kHz PCM).

3 Anechoic muzzle blast signal recording with higher sampling rate

One problem with interpreting real-world gunshot recordings is that the muzzle blast waves are reflected by the ground and other surrounding surfaces. The presence of overlapping direct and reflected waves at the microphone creates a complex recording that can be very difficult to interpret. Figure 2 shows a gunshot signal from a Glock 19 pistol recorded in a reverberant environment that exhibits tens of milliseconds of decaying echoes. As can be seen, it is difficult to identify the start and end of the muzzle blast duration from the reverberant recording [3].

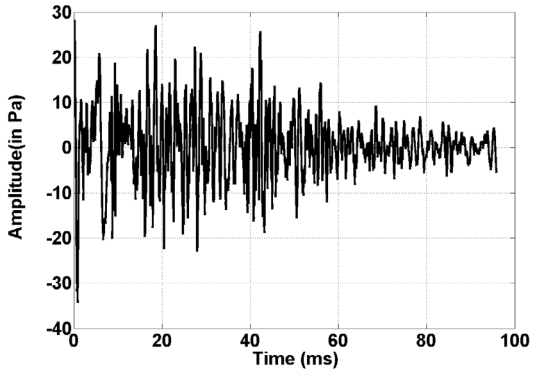

Figure 2: Reverberant gunshot signal with numerous surrounding reflections. Glock 19, 9 mm ammunition, 24-bit, 48 kHz PCM, with microphone distance 8 m, 90° off-axis.

Figure 3 shows a similar gunshot, but with the recording obtained in a quasi-anechoic environment. Although the muzzle blast portion is more clearly observed than in the reverberant recording of Figure 2, the detailed features of the muzzle blast signal still may not be discerned with the relatively low bandwidth and sampling rate of a conventional audio recorder.

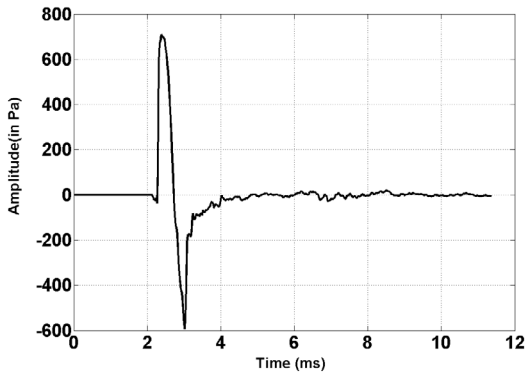

Figure 3: Anechoic recording of single gunshot, Glock 19, 9 mm ammunition, 24 bit, 44.1 kHz PCM, with microphone distance 8 m, 9◦ off axis.

Muzzle blast signals have an abrupt rising edge that occurs in microseconds, so a recording made with a

low sample rate and limited audio bandwidth may not include the extremely brief peak pressure spike and other waveform details.

Observing Figure 2 and Figure 3, it can be realized that the details of the muzzle blast are best captured in a quasi-anechoic environment with as high a sampling rate as possible. Figure 4 shows the recorded muzzle blast of the same Glock 19 handgun, but with a 500 kHz sampling rate and a microphone and amplifier with 200 kHz bandwidth (Frequency response ±1.0 dB @ gain ≤40 dB).

Here, the signal shows the fine details observed by the higher sampling rate and wider frequency range of the recording. Therefore, the gunshot recordings used in this investigation are obtained with a 500 kHz sampling rate. Furthermore, the shots were made from an elevated outdoor shooting platform with elevated microphones so that the full duration of the muzzle blast is recorded prior to the arrival of the first acoustic reflection from the ground [6].

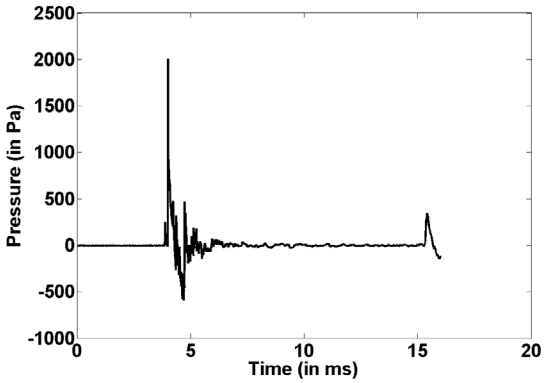

Figure 4: Anechoic recording of single gunshot, Glock 19 with 9 mm ammunition, 16-bit, 500 kHz PCM. Microphone distance 3 m, 98° off axis.

4 Defining muzzle blast duration

Hamernik and Hsueh [7] described the muzzle blast as a Friedlander wave. A Friedlander wave consists of an interval of over-pressure followed by an interval of under-pressure, as shown in Figure 5.

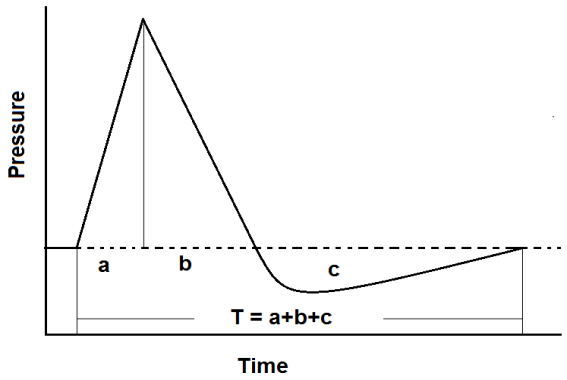

Figure 5: Friedlander assumption for describing muzzle blast shock wave characteristics [7]

As depicted, the total duration for the muzzle blast can be written as

$$T = a + b + c \quad . \tag{1}$$

We use two different approaches to determine the muzzle blast time intervals from gunshot audio recordings. One is a simple waveform observation approach, and the other is an energy accumulation approach.

The waveform observation approach uses the average pressure over the interval prior to the gunshot as the baseline, and then detects the points in the recorded waveform that cross the baseline. The duration is deemed to be the elapsed time between those points. The problem with this method is that the low-level waveform details vary sufficiently from shot to shot that even successive recordings of shots by the same firearm may give very different results. It is hard to conclude from the calculated duration whether the variance is due to external interference or naturally-chaotic differences between shots.

The energy accumulation approach is based on determining the time required for the accumulated acoustic energy to reach a certain percentage of the total muzzle blast energy calculated for the entire blast duration. This approach is based on the assumption that the integral of the squared pressure (proportional

to signal energy) will be a monotonically increasing function starting at zero, rising during the muzzle blast, and then levelling off as the muzzle blast dies away.

In both methods the long-term mean value is first deducted from the signal to eliminate any DC offset. A 16 ms portion of each muzzle blast recording is examined: 4 ms before the peak to 12 ms following the peak. It is ensured that none of the muzzle blast intervals included any reflections or ballistic shockwaves. The two methods for calculating the muzzle blast duration are described next.

4.1 Muzzle blast duration by waveform observation

- After selecting the 16 ms interval, identify the first sample, n_0, that crosses above the mean value (zero) prior to the peak.
- Identify the first sample, n_1, that crosses below the mean value (zero) after the signal has reached its peak.
- Determine the time interval between sample n_0 and n_1. This is the positive pressure interval ($a + b$).
- Identify n_2, the next sample in the waveform that crosses above the mean value following the negative peak of the waveform.
- Determine the time interval between sample n_1 and n_2. This is the negative pressure interval (c).
- These two durations are then added to get the calculated muzzle blast duration, T.

4.2 Muzzle blast duration by energy accumulation

- Choose the signal portion of interest according to the previously described process.
- Calculate the square of each sample value in the muzzle blast interval (proportional to signal power) and accumulate the total energy over the entire interval.
- Calculate the time required for the accumulated energy to reach a certain percentage of its final total. From empirical examination, 93% showed the best consistency for successive shots, so that has been the accumulation total chosen to define the duration for all firearms.

5 Methodology

To minimize reflections from nearby surfaces, the gunshot recording experiment was conducted in an open air environment at a ranch near Bozeman, Montana. The prime goal was to examine how the muzzle blast characteristics of a single shot vary as a function of azimuth from 0° (the line of fire) to 180° (behind the shooter). A total of twelve microphones were placed in a semi-circular arc with 3 meter radius covering this 180° azimuthal range. Framing was specially constructed to hold the microphones and maintain a nearly constant distance from the firing position. During all the shots the frame was kept constant (see Figure 6) [6].

The arrangement can be considered quasi-anechoic, as the closest significant reflecting surface was the ground, and both the microphones and the firearm were set at 3 meters above the surface. The path length difference between the direct sound and the first reflection from the ground provided at least 10 milliseconds time lag between the arrival of the direct and reflected waves [1].

Figure 6: 3 m elevated structure to create a quasi-anechoic platform covering 180° azimuth range.

5.1 Recording arrangement for gunshot signals

The choice of microphones was important for this experiment. The diameter of the diaphragm needed to be kept small enough to capture high frequency details of the signal. In this study, G.R.A.S. 40DP (diameter = 0.125 inches) condenser microphones were used. A total of twelve microphones were set. These microphones are relatively insensitive (some calibrated as low as 0.68 mV/Pa), so they had the capability of capturing the high sound pressure levels of interest. The other features included a wide frequency response (flat response from 6.5 Hz to nearly 70 kHz), and broad dynamic range (from 40 dB to 175 dB). The microphones were calibrated using a G.R.A.S. type 42AB calibrator at 250 Hz (114 dB SPL re 20μPa ref).

One G.R.A.S. 12AG and two G.R.A.S. 12AA amplifiers were used to amplify twelve different channels. 12 AG is an 8–channel amplifier module and the 12 AA are two-channel amplifiers. Among the twelve microphones, the first eight were connected to the 12 AG and the other four microphones were connected to the two 12AA modules, as depicted in Figure 7.

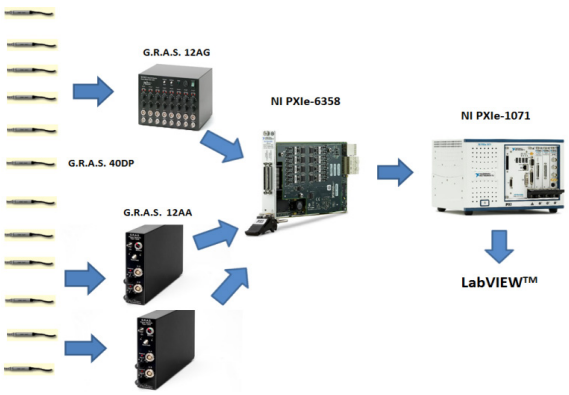

Figure 7: Experimental setup for simultaneous recording of 12 channels at 500 kHz sampling rate.

To capture the expected range of amplitudes, 20dB attenuators were used at the amplifier inputs. The 12AA has an inbuilt attenuation feature, but for the 12AG, external 20 dB attenuators were connected.

The signals were taken from the amplifier output and connected to a National Instruments (NI) multichannel data acquisition system. An NI PXIe-1071 PXI express chassis was used along with an NI PXIe-6358 data acquisition device (DAQ). This system can support up to 16 simultaneous analog inputs at 1.25 MS/s/channel with 16-bit resolution. For our analysis requiring 12 channels, we used eight channels on one slot and four on the other.

A custom program was implemented using LabVIEW to capture the gunshot signals. Sampling rates were 500 kilohertz per channel and signals from the twelve channels were captured simultaneously during each shot. It was expected that this high sampling rate would capture the very brief high pressure peaks of the muzzle blast signals. The acquisition mode was set to differential and the differential voltage range was specified between +5V to -5V. Following acquisition, the digital recordings were imported into MATLAB for post analysis.

5.2 Orientation of twelve G.R.A.S. 40DP microphones

The first microphone was placed adjacent to the line of fire (to avoid bullet hitting on the microphone). The other eleven covered 180 degrees azimuth (~16° angular spacing). To keep the distance from the shooting position to each sensor equal, variable length holders were used to position the microphones in a semicircular arc. Calibrated sensitivity measurements of the twelve microphones are given in Table 1.

Microphone	Sensitivity (in mV/Pa)	Microphone	Sensitivity (in mV/Pa)
01	0.90	07	0.90
02	0.68	08	0.84
03	0.85	09	0.91
04	0.88	10	0.75
05	0.84	11	0.84
06	0.69	12	0.82

Table 1: Measured microphone sensitivities.

Approximate angular positions of the microphones relative to the line of fire are shown in Figure 8.

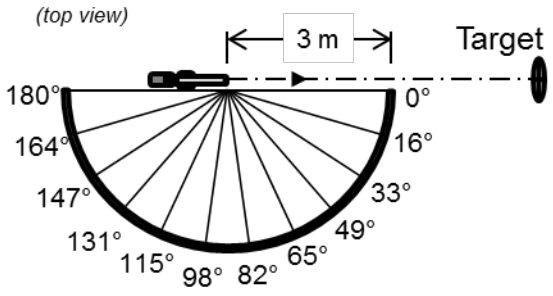

Figure 8: Angular position of twelve microphones with respect to the line of fire

6 Firearm Types

This study covered a range of commonly used firearms including shotgun, pistol, revolver, and rifle. Firearms and ammunition details are summarized in Table 2.

Firearm	Type	Ammunition	No. of shots observed
Remington 870	Shotgun	12 gauge 3 inch	3
CZ 452	Rifle	22 LR	10
Surgeon / AI	Rifle	308 Winchester	10
Colt 1911	Pistol	45 ACP	10
Glock 19	Pistol	9x19	10
Glock 23	Pistol	40 S&W	10
Sig 239	Pistol	357 Sig	10
Ruger SP101	Revolver	357 Magnum	9
Ruger SP101	Revolver	38 Special	10
Stag Arms AR15	Rifle	5.56 NATO	10

Table 2: Firearm and ammunition list for this experiment

7 Muzzle blast duration variation in different methods

Figure 9 shows the muzzle blast duration variation determined by the waveform observation method for 10 successive shots by a Sig 239 pistol fired with 125 grain jacketed hollow point bullets. As observed, there is shot-to-shot variation in muzzle blast durations (from 1.895 ms to 0.45 ms) when using the waveform observation method.

The recordings of the Sig 239 pistol also showed variability at different azimuths for a single shot. For example, the maximum and minimum duration varies from 1.834 ms to 0.632 ms for the first shot, as shown in Figure 10 (using waveform observation method) for the twelve microphone positions.

Figure 9: Muzzle blast duration variation Sig 239 pistol for ten consecutive shots with 125 gr Winchester JHP bullets (using waveform detection method).

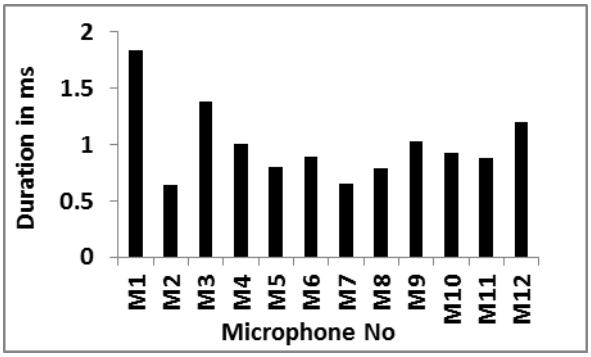

Figure 10: Azimuthal muzzle blast duration variation for a single shot from Sig 239 pistol with Winchester JHP bullets (using waveform detection method).

Similar analysis has been done for the Sig 239 with the energy accumulation method. As seen from Figure 11, for consecutive shots, there is better shot to shot consistency compared to the waveform observation method.

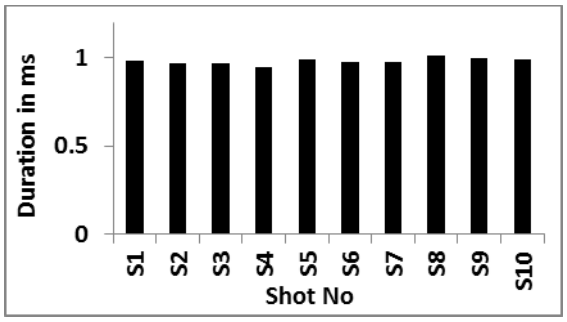

Figure 11: Muzzle blast duration variation Sig 239 pistol for consecutive shots with 125 gr Winchester JHP bullets (using energy accumulation method).

In Figure 12, the azimuthal variation for the first shot from the Sig 239 is calculated with the energy accumulation method. The highest duration was 1.248 ms, whereas the lowest was 0.844 ms.

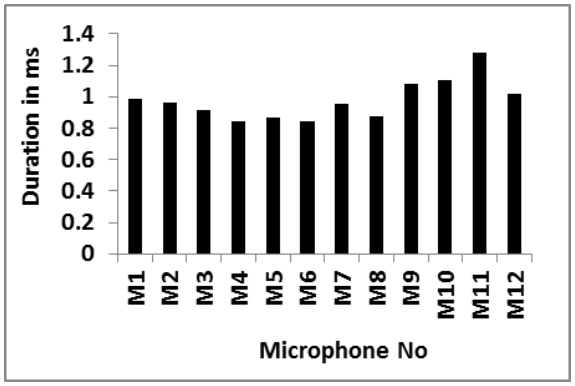

Figure 12: Azimuthal muzzle blast duration variation for a single shot from Sig 239 pistol with Winchester JHP bullets (using energy accumulation method).

Figure 13 shows the variation of in muzzle blast durations of the first shot for different firearms using the waveform observation technique. As seen from the figure, the Colt 45 records the highest duration. The Ruger SP 101 handgun was fired with two different types of ammunition: 38 special and 357 magnum; they exhibit different durations. The Glock 19 and Glock 23 are pistols that are physically very similar to each other but used different ammunition, resulting in blast duration differences.

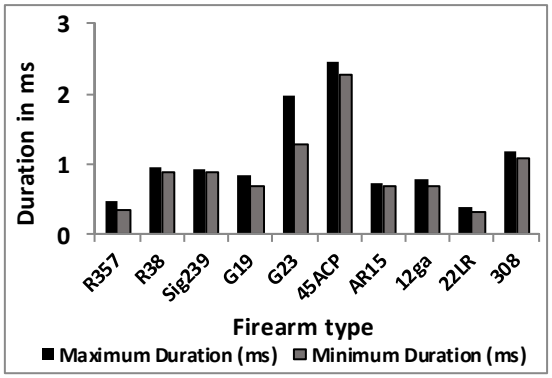

Figure 13: Maximum and minimum muzzle blast durations of different firearms on-axis based on waveform observation method (for ten shots).

Similar diversity in durations is also observed with the energy accumulation method. Figure 14 depicts azimuthal shot-to-shot variation for several firearms using the energy accumulation method. The durations differ considerably from the waveform observation method. The highest duration was observed for the shotgun category. As seen from the analysis, there are also duration contrasts in multiple shots from a single firearm.

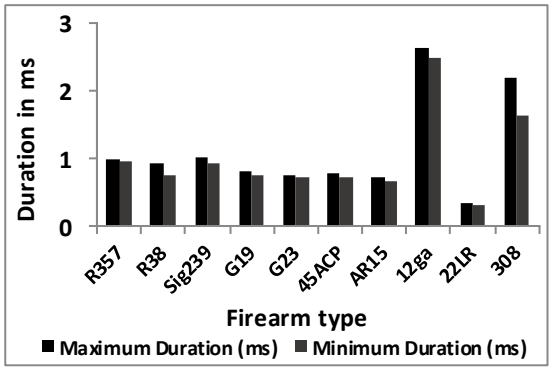

Figure 14: Maximum and minimum muzzle blast durations of different firearms at the line of fire based on 93% of total muzzle blast energy (for 10 shots)

8 Comparing waveform observation and energy accumulation methods

In our recordings, the muzzle blast shows non-uniformity from one shot to another even when the same firearm and ammunition are used. These differences may be the natural acoustical characteristics of firearms, or it can happen due to some kind of atmospheric disturbances at the time of the recording: wind, background noise, or convection. The presence of noise may affect the calculated duration in several ways, especially when performing waveform observation of zero-crossings. For example, the muzzle blast signals recorded by M2 (16°) and M3 (33°) for a shot fired from the Sig 239 pistol are shown in Figure 15. The signal exhibits several undulations for M2 (upper subplot) that cross the base level much earlier than the observation for M3 (lower subplot), causing the two calculated muzzle blast durations to be quite different even for the neighboring microphones: 0.636 ms for M2 and 1.378 ms for M3.

When we calculated the durations with the energy accumulation method, the values were 0.96 ms and 0.918 ms, respectively (a difference of 0.042 ms).

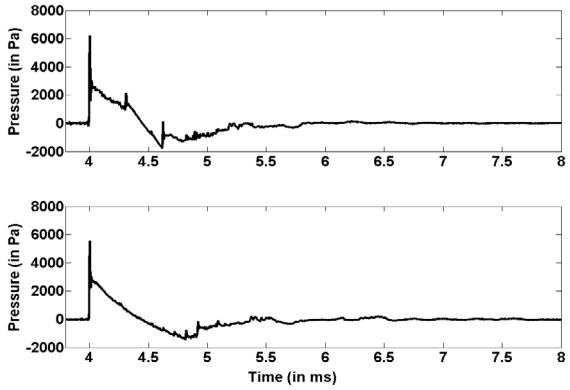

Figure 15: Muzzle blast waveform at 3m distance for S1 of sig 239 at M2 and M3.

Again for the Sig 239 firearm, we examined muzzle blast waveforms for shot 6 at microphone 11 (upper subplot) and microphone 12 (lower subplot) in Figure 16. The blast signal at M12 exhibits a smaller peak before reaching to the highest peak. This peak contributes greatly to the total energy accumulation and results in a smaller muzzle blast duration measured by the energy accumulation method (0.89 ms compared to 1.548 ms at M11). When we applied the waveform observation method, the durations were 0.816 ms and 1.044 ms. The difference was smaller (0.228 ms) than the earlier method (0.658 ms).

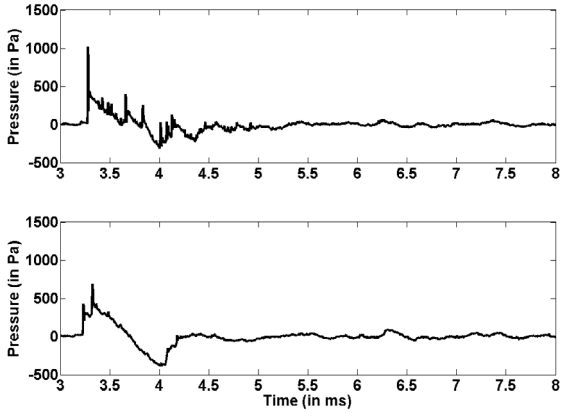

Figure 16: Muzzle blast waveform at 3m distance for S6 of sig 239 at M11 and M12.

We have observed the muzzle blast waves for the Glock 23 pistol on-axis for several different shots. As seen from Figure 17, the waveform for shot 3 reaches the base (zero) value much earlier than shot 2 or shot 4.

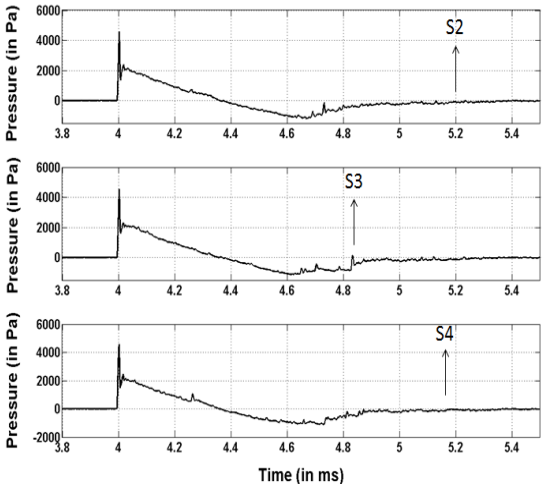

Figure 17: Muzzle blast pressure wave at the line of fire for 3 different shots fired with the Glock 23 pistol.

The blast durations determined by applying the waveform observation method were 1.412 ms, 0.842 ms and 1.382 ms, respectively, compared to 0.748 ms, 0.734 ms and 0.772 ms via the energy accumulation method.

Based on these empirical observations, we conclude that at lower azimuths, where there are high frequency fluctuations that can cause the waveform to cross the base level earlier or later in time, it is more consistent to use the energy accumulation method, as it is less sensitive to the effect of any sudden change of voltage values. At higher azimuths, where the muzzle blast sound levels are lower, the waveform observation method provides good consistency for determining the blast durations.

9 Energy accumulation for several firearms

The nature of energy accumulations were observed for the first shot at the line of fire for all the firearms using the calculation described earlier in section 4.2.

As an example, a muzzle blast recording for the 12 gauge shotgun is shown in Figure 18, and the corresponding energy accumulation is shown in Figure 19. The horizontal lines indicate the 90% and 95% levels.

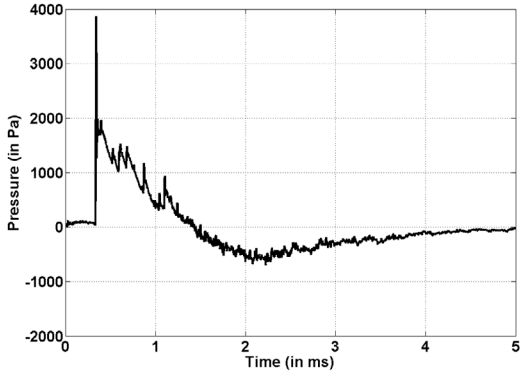

Figure 18: Muzzle blast waveform on-axis for the 12 gauge shotgun.

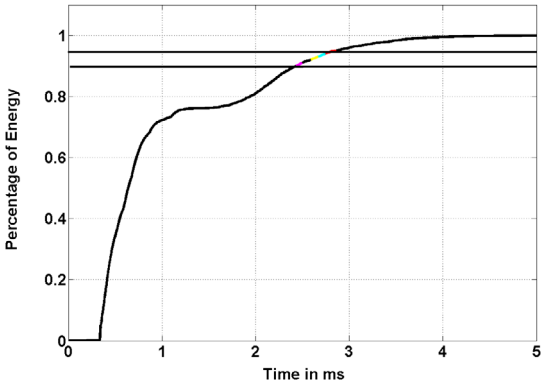

Figure 19: Energy accumulation during the muzzle blast period for the 12 gauge shotgun (horizontal lines indicate the 90% and 95% levels).

Figure 20 shows example energy accumulation characteristics calculated for the other firearms. Again, the transition region from 90% of the total energy to 95% is marked by the two horizontal lines. As observed, there are noticeable differences from one type of firearm to the other. It can be observed that the rate of rise in accumulated energy is more rapid for the handguns than for the rifles and shotguns. The slowest rise of accumulated energy was for the shotgun.

For all the cases, there is an abrupt initial rise in accumulated energy during the impulsive peak of the muzzle blast, followed by a more gradual plateau interval as the negative phase of the muzzle blast decays back toward zero. As detected, the duration of the plateau interval was found to be longer for the rifles and the shotgun compared to the handguns.

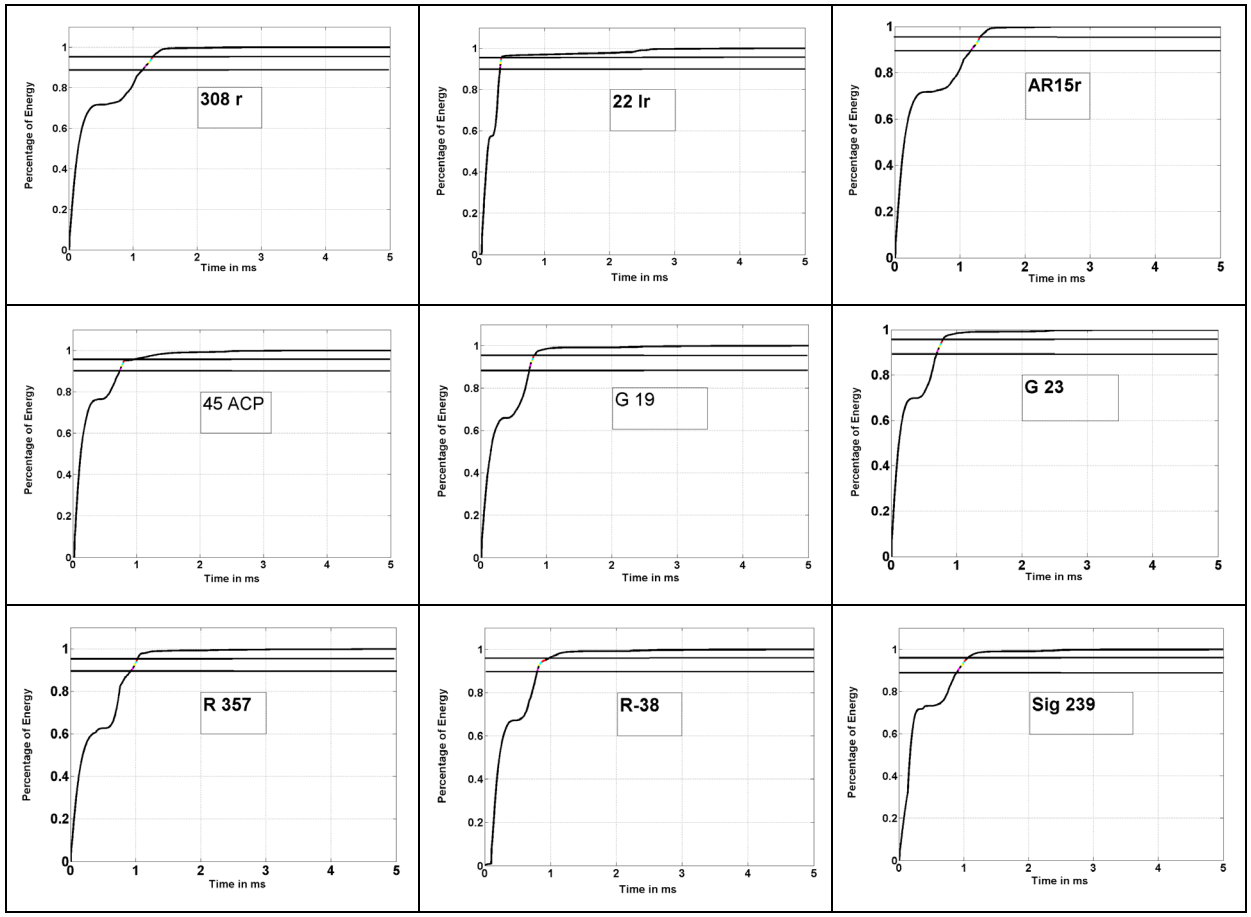

Figure 20: Energy accumulation for the first 5 milliseconds of the muzzle blast signal for several firearms.

10 Total acoustic energy variation for different firearms

After firing, the muzzle blast acoustical energy propagates in all directions. Figure 21 shows the spherical geometry surrounding the muzzle.

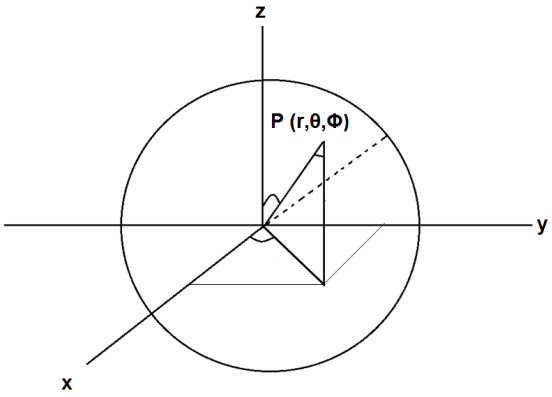

Figure 21: Spherical geometry for acoustical propagation of the muzzle blast.

The energy formula for spherical propagation is

$$E_{total} = \int_{\theta=0}^{\theta=2\pi} \int_{\emptyset=0}^{\emptyset=\pi} \int_{r=0}^{r=R} r^2 I(\theta)\, dr d\emptyset d\theta \qquad (2)$$

where R = 3 meter.

In our experiment, we have found that the muzzle blast energy does not emanate equally in a spherical fashion, but rather depends on azimuth. The energy is calculated from 0° to 180° for θ in the horizontal plane of the microphones, and then rotated cylindrically over 360° in ϕ to achieve a three dimensional total.

With discrete data, our energy equation becomes

$$E_{total} = 2\pi R^2 \sum sin\theta d\theta \qquad (3)$$

The variations of acoustical energy in different shots is shown in Figure 22. As expected, the rifle category shows the highest acoustical energy totals—except for the 0.22 caliber rifle with rim fire bullets. The shotgun, 308, and AR15 firearms produce significantly higher acoustic energy than the handguns.

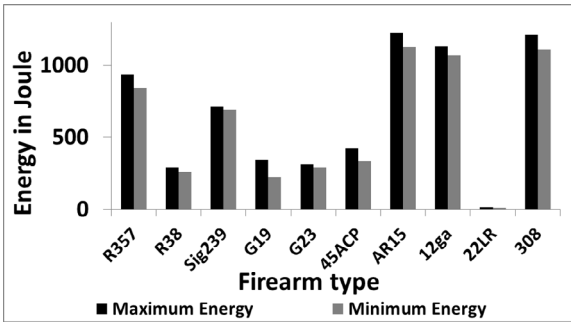

Figure 22: Total acoustic energy variation of different firearms for consecutive shots.

11 CONCLUSIONS

In our experiment we observe that muzzle blast durations show azimuthal variation for a single shot, and also vary in duration from one shot to another for successive shots by the same firearm, or for the same firearm fired with different ammunition. Comparing the waveform observation and energy accumulation methods for calculating the muzzle blast durations, we find that each approach has pros and cons. The rate of rise of energy during the muzzle blast duration also depends on the firearm type, as does the total acoustical energy estimated for successive shots.

The ammunition used in this experiment was commercially prepared, but we did not specify match grade bullets. Moreover, the firearms were hand-held by a competent marksman, but the exact location of the muzzle may have varied from one shot to another as the marksman repositioned the gun after each successive shot. For future studies we expect to consider the effect of these physical variables, as well as using a wider variety of firearms and ammunition.

12 ACKNOWLEDGEMENTS

This research work is supported by the National Institute of Justice (Award: 2014-DN-BX-K034) for Research and Development in Forensic Science for Criminal Justice Purposes. We would like to thank Dr. Steven Shaw, Professor, Electrical & Computer Engineering, Montana State University, and Angelo Borzino, Lieutenant Colonel, Military Engineering

Institute, Rio de Janeiro, Brazil, for their support with our gunshot recordings and interpretation.

References

[1] R.C. Maher and S.R. Shaw, "Directional aspects of forensic gunshot recordings," *Proc. AES 39th International Conf.: Audio Forensics: Practices and Challenges*, Hillerød, Denmark, 2010.

[2] R.C. Maher, "Lending an ear in the courtroom: forensic acoustics," *Acoustics Today*, 11(3), pp. 22-29, 2015.

[3] R.C. Maher and S.R. Shaw, "Gunshot recordings from digital voice recorders," *Proc. AES 54th International Conf.: Audio Forensics – Techniques, Technologies, and Practice*, London, U.K., 2014.

[4] R.C. Maher and S.R Shaw, "Deciphering gunshot recordings," *Proc. AES 33rd International Conf.: Audio Forensics – Theory and Practice*, Denver, CO, 2008.

[5] G. Klingenberg, "Gun muzzle blast and flash," *Propellants, Explosives, Pyrotechnics*, 14(2), pp. 57–68, 1989. http://doi.org/10.1002/prep.19890140204

[6] R.C. Maher and T.K. Routh, "Advancing forensic analysis of gunshot acoustics," Preprint 9471, *Proc. 139th Audio Engineering Society Convention*, New York, NY, 2015.

[7] R.P. Hamernik and K.D.Hsueh, "Impulse noise: some definitions, physical acoustics and other considerations," *J. Acoust. Soc. Am.*, 90(1), pp. 189-196, 1991. http://doi.org/10.1121/1.401287